Science of the Total Environment 910 (2024) 168684

Contents lists available at ScienceDirect

Science of the Total Environment

journal homepage: www.elsevier.com/locate/scitotenv

Temporal and spatial variations of air-sea CO_2 fluxes and their key influence factors in seagrass meadows of Hainan Island, South China Sea

Songlin Liu [a,b,c,d], Jiening Liang [a,b,c,d], Zhijian Jiang [a,b,c,d], Jinlong Li [a,b,c,d], Yunchao Wu [a,b,d], Yang Fang [a,b,c,d], Yuzheng Ren [a,b,c,d], Xia Zhang [a,b,d], Xiaoping Huang [a,b,c,d,*], Peter I. Macreadie [e]

[a] Key Laboratory of Tropical Marine Bio-resources and Ecology, South China Sea Institute of Oceanology, Chinese Academy of Sciences, Guangzhou 510301, China
[b] Sanya Institute of Ocean Eco-Environmental Engineering, Sanya 572100, China
[c] University of Chinese Academy of Sciences, Beijing 100049, China
[d] Guangdong Provincial Key Laboratory of Applied Marine Biology, South China Sea Institute of Oceanology, Chinese Academy of Sciences, Guangzhou 510301, China
[e] Centre for Integrative Ecology, School of Life and Environmental Sciences, Deakin University, Burwood, Victoria 3125, Australia

HIGHLIGHTS

- Air-sea CO_2 fluxes of tropical seagrass ecosystems were observed.
- Seawater pCO_2 was mainly mediated by biological effects.
- All seasons showed net uptake CO_2, with exception of summer.
- Annual air-sea CO_2 flux of the tropical seagrasses was -0.635 mol m^{-2} yr^{-1}.
- Nutrient pollution caused a 23–54 % decline in CO_2 uptake by seagrasses.

GRAPHICAL ABSTRACT

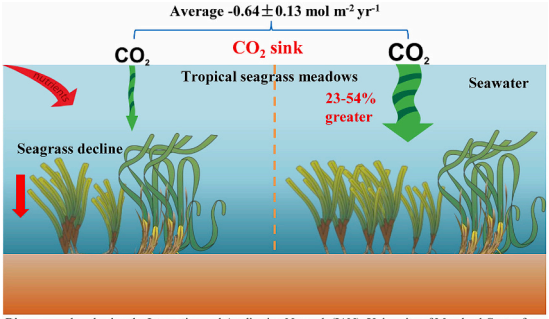

Diagram produced using the Integration and Application Network (IAN), University of Maryland Center for Environmental Science, Cambridge, Maryland.

ARTICLE INFO

Editor: Jan Vymazal

Keywords:
Air-sea CO_2 flux
Seagrass ecosystems
Carbon neutrality
Blue carbon
Eutrophication
Carbon budget

ABSTRACT

Seagrass ecosystems have received a great deal of attention for contributing to uptake of atmospheric CO_2, and thereby helping to mitigate global climate change ('blue carbon'). Carbon budgets for seagrass ecosystems are developed by estimating air-sea CO_2 fluxes. Data for air-sea CO_2 flux for tropical seagrass ecosystems are lacking, which is problematic for constraining global seagrass carbon budgets. Here, we sought to address this important data gap for tropical seagrass ecosystems (dominated by *Thalassia hemprichii* and *Enhalus acoroides*) from the Hainan Island of South China Sea, while also testing what the main factors driving the variations of air-sea CO_2 fluxes are. We found that air-sea CO_2 fluxes exhibited a U-shape diurnal variability from 6 a.m. to 6 a.m. of the next day, with the highest and lowest air-sea CO_2 fluxes values at early morning and afternoon, respectively. Biological processes were the driving force for mediating diurnal variations of seawater pCO_2. The $pCO_{2,\ sea}$ in different seasons displayed a trend of increasing from spring, reaching maximum in summer and then a decreasing trend after summer, where water temperature, wind speed and seagrass growth mainly drove the variations. This resulted in net uptake of CO_2 in all seasons except during summer in our study seagrass

* Corresponding author at: South China Sea Institute of Oceanology, Chinese Academy of Sciences, Guangzhou 510301, China.
E-mail address: xphuang@scsio.ac.cn (X. Huang).

https://doi.org/10.1016/j.scitotenv.2023.168684
Received 20 November 2022; Received in revised form 13 November 2023; Accepted 16 November 2023
Available online 18 November 2023

ecosystems, with greater negative values found in autumn (−3.63 ± 0.76 mmol m^{-2} d^{-1}) than those in winter (−2.84 ± 0.60 mmol m^{-2} d^{-1}). While the nutrient loading induced seagrass biomass changes (especially the seagrass *T. hemprichii*), which mediated the air-sea CO_2 fluxes changes among different seagrass meadows. Net annual CO_2 uptake potential under low nutrient loading (−0.77 ± 0.16 mol m^{-2} yr^{-1}) was 23–54 % greater than high nutrient loading seagrass meadows, with the average annual air-sea CO_2 flux of the three seagrass meadows as −0.64 ± 0.13 mol m^{-2} yr^{-1}. These results suggest that tropical seagrass meadows of Hainan Island are a significant CO_2 sink of atmospheric CO_2, but this capacity can be diminished by nutrient loading. Scaling up, we estimate the annual atmospheric CO_2 uptake by seagrass meadows of Hainan Island (total area 55.28 km^2) was 1544 t of CO_2 yr^{-1}, equivalent to the annual emissions from the wholesale, retail, accommodation and catering industries of 164,000 tourists in Hainan Island. With carbon neutrality becoming an important part of global climate governance, this study provides timely information for capitalising on the ability of seagrasses to contribute to natural climate solutions.

1. Introduction

Global average atmospheric carbon dioxide (CO_2) concentrations have reached ~420 parts per million (ppm; https://gml.noaa.gov/ccgg/trends/gl_trend.html accessed October 2023), which is >50 % higher than pre-industrial concentrations. Seagrass meadows, commonly referred to as 'blue carbon' ecosystems, have high primary productivity (817 g C m^{-2} per year) which means they reduce atmospheric CO_2 and act as carbon sinks (Duarte et al., 2013; Macreadie et al., 2021; Mateo et al., 2006). CO_2 will be bound to primary producers in seagrass ecosystems (including seagrass, epiphyte, macroalgae, phytoplankton and microphytobenthos) and converted into the biomass of body tissues through photosynthesis. This will then be sequestrated in the sediments for the long term through a series of physical, chemical and biological processes (Macreadie et al., 2014; Mcleod et al., 2011; Tang et al., 2018). Air-sea CO_2 flux measurements underpin carbon budgets in seagrass ecosystems, and can validate strategies for using blue carbon as a natural climate solution (Macreadie et al., 2019).

Air-sea CO_2 fluxes within seagrass ecosystems are diurnally-variable, with tidal immersion and solar radiation shown to be key drivers of this variation (Bahlmann et al., 2015; Ollivier et al., 2022). Air-sea CO_2 fluxes that are influenced by tide are mainly attributed to changes in gas diffusion and advective exchange processes (Bahlmann et al., 2015), while light intensity affects net ecosystem production changes (Berg et al., 2019). In a *Zostera noltii* meadow of Ria Formosa lagoon, the average values of air-sea CO_2 fluxes in the daytime during immersion and air exposure were found to be −16.4 mmol m^{-2} h^{-1} and −9.1 mmol m^{-2} h^{-1} (negative value represents inflow of CO_2 from atmospheric), respectively, while at night were observed to be 20.1 mmol m^{-2} h^{-1} and 8.4 mmol m^{-2} h^{-1} (positive value represents outflow of CO_2 into the atmosphere), respectively (Bahlmann et al., 2015). Temperature, terrestrial inputs and net ecosystem production were the key factors mediating the seasonal air-sea CO_2 flux variations in seagrass ecosystems (Gazeau et al., 2005; Jiang et al., 2008; Kim et al., 2015; Tokoro et al., 2014). Increasing seawater temperature decreases the CO_2 solubility (increasing the partial pressure of carbon dioxide, i.e. pCO_2), and may enhance the release of CO_2 into the atmosphere, while colder seawater increases the CO_2 solubility and dissolves more CO_2 from the atmosphere (Takahashi et al., 2002). The dissolved organic carbon and dissolved inorganic carbon of terrestrial inputs during wet seasons are abundant in coastal ecosystems, increasing the pCO_2, which may consequently enhance the release of CO_2 into the atmosphere (Banerjee et al., 2018; Jiang et al., 2008). For example, the CO_2 fluxes of Chilika Lagoon seagrass ecosystem in dry and wet seasons were −33.9 mmol m^{-2} d^{-1}-21.1 mmol m^{-2} d^{-1} and 3.11 mmol m^{-2} d^{-1} - 29.8 mmol m^{-2} d^{-1}, respectively (Banerjee et al., 2018). The higher positive CO_2 fluxes values were induced by terrestrial inputs of organic detritus with stimulating heterotrophic remineralization during wet seasons (Banerjee et al., 2018). Further, net ecosystem production contributes much to the assimilation of atmospheric CO_2 by changing the balance of total alkalinity and dissolved inorganic carbon in the air-sea CO_2 flux (Banerjee et al., 2018; Tokoro et al., 2014). The average air-sea CO_2 flux was −1.46 ± 0.38 μmol m^{-2} s^{-1} during the growing season in a *Zostera marina* meadow of Furen lagoon, Japan, while positive fluxes (0.42 ± 0.15 μmol m^{-2} s^{-1}) were observed during autumn (decay) season from September to November (Tokoro et al., 2014). Previous studies have mainly focused on the characteristics of air-sea CO_2 flux in different seasons of seagrass ecosystems. However, there is still little information about the comprehensive driving factors for air-sea CO_2 flux variations of different seasons.

Further, air-sea CO_2 fluxes in different seagrass ecosystems exhibit strong spatial heterogeneity due to the variations of environmental and biological factors (Bauer et al., 2013; Tokoro et al., 2014; Van Dam et al., 2021a). At a global scale, Van Dam et al. (2021a) reported that the seagrass ecosystems of Bob Allen Keys of USA and Östergarnsholm of Sweden were net CO_2 sources, while Estero EI Soldado of Mexico and Furen Lagoon of Japan were strong CO_2 sinks. Even in a relative fine-scale region, obvious air-sea CO_2 flux differences were observed (Tokoro et al., 2014; Van Dam et al., 2019). For example, the average air-sea CO_2 fluxes in high density and low density *Thalassia testudinum* meadows of Florida Bay were 0.38 mmol m^{-2} h^{-1} and 0.13 mmol m^{-2} h^{-1}, respectively (Van Dam et al., 2019). While the air-sea CO_2 flux measurements over seagrass ecosystems have developed for a decade (Polsenaere et al., 2012), previous studies have mainly focused on the temperate North American (Mexico and American), Western and Southern European (Portugal, France and Spain), Japan, and southern Australia regions (Bahlmann et al., 2015; Champenois and Borges, 2021; Ollivier et al., 2022; Van Dam et al., 2021a). With a significant lack of case studies on the air-sea CO_2 flux of tropical seagrass ecosystems, this knowledge gap on the air-sea CO_2 flux from seagrass ecosystems limits our capacity to formulate strategies to mitigate climate change.

It has been reported by Stankovic et al. (2021) that the seagrass meadows in the Tropical Indo-Pacific Bioregion are hotpots for carbon sequestration, with the annual organic carbon accumulation rate as much as 5.85–6.80 Tg C $year^{-1}$. Tropical seagrass meadows of China are mainly distributed along the coastline of Hainan Island in the South China Sea, with presenting the most abundant seagrass biodiversity (Jiang et al., 2017). Although many previous studies have reported the carbon storage potential and sequestration rate in tropical seagrass meadows of China (Fu et al., 2021; Jiang et al., 2018; Jiang et al., 2017), data on air-sea CO_2 flux in tropical seagrass ecosystems of China are still lacking. In this study, we carried out the air-sea CO_2 fluxes measurements in tropical seagrass ecosystems of Hainan Island, South China Sea, over different seasons. Further, we measured seagrass biomass and seawater nutrients to help explain the major biological and environmental conditions influencing air-sea CO_2 flux in seagrass ecosystems. Overall, this study fills an important data gap in the temporal source-sink dynamics of China's tropical seagrass, which is critical for developing the carbon budget for China's seagrass ecosystems.

2. Materials and methods

2.1. Study site

Three seagrass meadows in Tanmen Harbor, Li'an Bay and Xincun Bay, located along the eastern coastline of Hainan Island, South China Sea, were our study areas (Fig. 1). Each seagrass meadow was set up with one sampling station, where the longitude and latitude of the sampling stations in Tanmen, Li'an and Xincun were 110.6347° E and 19.2503° N, 110.044° E and 18.4266° N, and 109.9862° E and 18.4043° N, respectively (Fig. 1). Li'an Bay and Xincun Bay are sandy sediment lagoons with only one narrow channel connecting to the open water, while Tanmen Harbor is a reef flat sediment open water bay. The dominant seagrass species at these three seagrass ecosystems are *Thalassia hemprichii* and *Enhalus acoroides* and are distributed in the shallow waters of each site with depths of <2 m. These are mixed-seagrass meadows with *T. hemprichii* and *E. acoroides* occupying different patches alongside each other. The tides in these three seagrass meadows are dominated by irregular diurnal type, with typical average tidal ranges as 0.7– 0.8 m (Huang et al., 2020; Li et al., 2014). Tourism and marine aquaculture are developed in Xincun Bay, with large nutrient inputs from aquaculture and sewage discharge, while Li'an Bay has less aquaculture area and sewage discharge in comparison (Huang et al., 2020). In contrast, Tanmen Harbor is an open bay that is less impacted by human activities (Zhang et al., 2022). According to our previous studies, the seawater temperature, salinity, pH and dissolved oxygen were similar among the three seagrass ecosystems, while the nutrient loading levels varied, with Xincun having the highest levels of nutrients, followed by Li'an, and then Tanmen (Liu et al., 2020).

2.2. Field sampling

In January 2021 (winter), May 2021 (spring), August 2021 (summer) and November 2021 (autumn), seawater pCO_2 ($pCO_{2,\ sea}$), atmospheric pCO_2 ($pCO_{2,\ atm}$), seawater temperature, salinity and wind speed were continuously measured for >24 h at the same sampling station of each seagrass ecosystem (each meadow was set up with one sampling station) (Fig. 1).

The $pCO_{2,\ sea}$ and $pCO_{2,\ atm}$ were measured with a Pro-Oceanus CO_2-Pro Atmosphere from Pro-Oceanus Systems Inc., which were determined by a non-dispersive infrared detector. A CO_2-Pro Atmosphere is equipped with an accurate in situ submersible pCO_2 sensor, an air-side waterproof NEMA box and a water pump (Seabird Inc.). The accuracy and resolution of the sensor were 0.5 % and 0.01 ppm, respectively. The measurement detection range is 0– 1000 ppm, and the operation temperature range is 15–45 °C. The water pump and air-side box allowed for $pCO_{2,\ sea}$ and $pCO_{2,\ atm}$ measurements to be made in the single pCO_2 sensor by directly drawing samples from surrounding seawater and above sea surface air, respectively. The water pump was connected to the sensor water inlet barbed connector and back of the sensor using 3/8″-1/2″ ID tubing and a 2-pin underwater cable, which were mounted on a buoy underwater at a depth of 0.5 m. The air-side waterproof NEMA box was connected to the sensor by tygon tubing for air intake and air exhaust, and was mounted on the buoy at 0.5 m above the sea surface. The instrument was powered with an external battery pack fixed on the buoy at 1.0 m above the sea surface. During a sampling period, a buoy equipped with a Pro-Oceanus CO_2-Pro Atmosphere instrument was transported to the same sampling station of each seagrass ecosystem by a skiff before 6 a.m., and the buoy was then moored to the sediment by an anchor chain for $pCO_{2,\ sea}$ and $pCO_{2,\ atm}$ data collection. Continuous mode set to record every second was applied for $pCO_{2,\ sea}$ and $pCO_{2,\ atm}$ measurements, time between $pCO_{2,\ atm}$ measurements was selected as

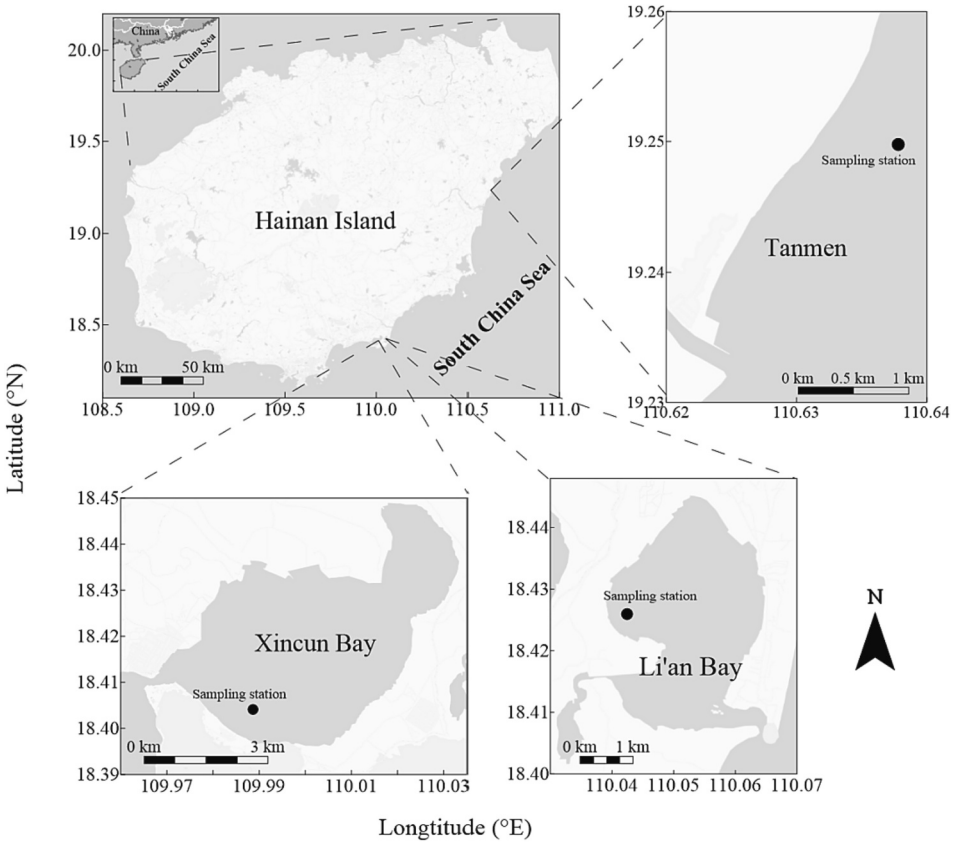

Fig. 1. Study areas and sampling stations of Xincun, Li'an and Tanmen in Hainan Island, South China Sea.

10 min (6 min and 4 min for $pCO_{2,\ sea}$ and $pCO_{2,\ atm}$ measurements, respectively), and between zero point corrections interval was set as 4 h. A hand-held anemometer (WS-30, Nanjing Shengrong Instrument Equipment *Co*. Ltd) was mounted on the buoy at 1.0 m above the sea surface, and the wind speed was recorded every minute (measurement accuracy set as 6 %). Additionally, physicochemical parameters of seawater temperature and salinity were measured in-situ at one-minute intervals using a HydroCAT Conductivity-Temperature-Depth (CTD) meter (Sea-Bird Coastal, USA), with the meter fixed to the anchor chain. The buoy and the CTD were used after for 24 h in the sampling station of each seagrass meadow (each seagrass meadow was set up one sampling station) with the sampling period set from 6 a.m. to 6 a.m. the next day. We then transported this to the other seagrass ecosystems for further diurnal $pCO_{2,\ sea}$, $pCO_{2,\ atm}$, wind speed, seawater temperature and salinity data collection.

After collecting physiochemical parameters, around the sampling station where the buoy was placed (within 50 m distance), four duplicates of 1 L seawater were collected, and four quadrats (0.25 m^2) of *T. hemprichii* and *E. acoroides* shoot densities were determined by counting the shoots of the different species. All seagrass leaves in the quadrats were then collected for subsequent analysis. Collected seawater was filtered onto pre-combusted GF/F filters (Whatman, 500 °C, 3 h) and stored in a brown ampoule bottle. Collected seagrass leaves were cleaned using in situ seawater to remove detritus and epiphytes, and stored in transparent zip-lock plastic bags. All samples were frozen and then transported to the laboratory for subsequent analysis.

2.3. Nutrients and seagrass biomass measurement

The filtered seawater was analyzed for concentrations of ammonium (NH_4–N), nitrate (NO_3–N), nitrite (NO_2–N), and phosphate (PO_4–P) using a continuous flow analytic system (SEAL Analytical AA3, SEAL Analytical GmbH, Norderstadt, Germany). Dissolved inorganic nitrogen (DIN) was represented as total content of ammonium, nitrate and nitrite, while dissolved inorganic phosphate (DIP) content was represented as phosphate. The seagrass leaf samples were dried at 60 °C for 48 h and weighed for dry weight (DW). The seagrass leaf weight was then converted to biomass per square meter.

2.4. Determination of air-sea CO_2 flux

Firstly, the average values of every 10 min for $pCO_{2,\ sea}$, $pCO_{2,\ atm}$, wind velocity at 1 m in height above the sea surface (μ_1, m s^{-1}) seawater temperature (T, °C) and salinity (S, ‰) were calculated. Then, air-sea CO_2 fluxes (F_{CO_2}) were calculated according the following equation:

$$F_{CO_2} = k \times k_0 \times \Delta pCO_2 \tag{1}$$

where k is the gas transfer velocity of CO_2, k_0 (mol L^{-1} atm^{-1}) is the temperature and salinity dependent solubility coefficients (Weiss, 1974) and ΔpCO_2 is the difference in partial pressure of CO_2 between seawater and air ($pCO_{2,\ sea}$ - $pCO_{2,\ atm}$, μatm).

To calculate k (cm h^{-1}), we used the wind-based gas transfer parametrization of Wanninkhof (2014):

$$k = 0.251 \times \mu_{10}^2 \times (Sc/660)^{-0.5} \tag{2}$$

where *Sc* is the Schmidt number of CO_2 calculated as a function of temperature and salinity according to Wanninkhof (2014):

$$Sc = 2116.8 - 136.25 \times T + 4.7353 \times T^2 - 0.092307 \times T^3 + 0.0007555 \times T^4 \tag{3}$$

The μ_{10} (m s^{-1}) is wind speed at a height of 10 m above sea surface that calculated with μ_1 based on (Sutton et al., 2017):

$$\mu_{10} = \frac{\mu_z}{1 + \frac{\sqrt{Cd10}}{0.4} \times ln\left(\frac{z}{10}\right)} \tag{4}$$

where *z* is the height (m) of the wind sensor, u_z is wind speed in m s^{-1} recorded by the moored sensor, Cd_{10} is the drag coefficient of 0.0011, and 0.4 is von Karman's constant.

As the average data per 10 min were used for F_{CO_2} calculation, we converted this to the F_{CO_2} per minute (μmol m^{-2} min^{-1}) assuming the fluxes were similar within 10 min. Diurnal air-sea CO_2 fluxes ($F_{CO_{2,day}}$) were calculated by summing all the instantaneous (minutes) fluxes determined each day. Annual CO_2 fluxes ($F_{CO_{2,year}}$) at each seagrass ecosystem were estimated by taking the average of the four seasons' diurnal fluxes, then multiplying by 365 days per year. Positive air-sea CO_2 fluxes values indicate gas fluxes from water to the atmosphere, while negative values indicate fluxes from the atmosphere to water.

Next, we estimated the uncertainty of F_{CO_2} (δF_{CO_2}) from errors for three variables k, k_0, and ΔpCO_2 (defined, as δk; δk_0, and $\delta\Delta pCO_2$, respectively). The uncertainty of k_0 is about 0.3 % (Weiss, 1974), while the $\delta\Delta pCO_2$ is 1 %, as the accuracy of the pCO_2 sensor was 0.5 %. For δk estimation, which includes the uncertainty of 10 % in the coefficient of 0.251, there was 5 % uncertainty in *Sc* (Wanninkhof, 2014), and 6 % in in situ wind speed. We assume that the uncertainty for these three parameters is independent, and the δF_{CO_2} can be calculated as follows:

$$\delta F_{CO_2} = \sqrt{\delta_k^2 + \delta_{k0}^2 + \delta_{\Delta pCO2}^2} == \sqrt{0.003^2 + 0.01^2 + 0.21^2} \approx 0.21$$

Therefore, the uncertainty of F_{CO_2} is approximately 21 % and determined mainly by the uncertainty of k.

2.5. Biological and temperature control in $pCO_{2,\ sea}$ calculations

$pCO_{2,\ sea}$ is affected by temperature, physical processes (horizontal and vertical mixing), and biological processes (Ávila-López et al., 2017; Barrón et al., 2006). Since these three seagrass meadows have a water depth < 2 m, with well-mixed vertical water and oceanic dominated embayment with no river directly inputting to these seagrass meadows, the effects of horizontal mixing and vertical mixing on $pCO_{2,\ sea}$ were minor. We assumed that the diurnal changes of observed of $pCO_{2,\ sea}$ would result mostly from temperature and biological effects. Temperature and biological effect $pCO_{2,\ sea}$ in seawater has been calculated following the procedure described by Takahashi et al. (2002). To remove the temperature effect from the observed $pCO_{2,\ sea}$ ($pCO_{2\ obs}$), the $pCO_{2\ obs}$ values were normalized to mean temperature $pCO_{2,\ sea}$ ($pCO_2\ T_{mean}$) during the investigated period:

$$pCO_2\ T_{mean} = pCO_{2\ obs} * exp[0.0423 * (T_{mean} - T_{obs})] \tag{5}$$

where $pCO_{2\ obs}$ is the observed $pCO_{2,\ sea}$ at in situ temperature and T_{obs} is the measured temperature and T_{mean} is the mean surface temperature of the investigated period. For each site seasonal biological effect $pCO_{2,\ sea}$ was calculated as Eq. (6):

$$(\Delta pCO_2)_{bio} = (pCO_2\ T_{mean})_{max} - (pCO_2\ T_{mean})_{min} \tag{6}$$

While the effect of temperature on $pCO_{2\ obs}$ was calculated as described in Eq. (7):

$$pCO_2\ T_{obs} = pCO_{2\ mean} * exp\ [0.0423(T_{obs} - T_{mean})] \tag{7}$$

where $pCO_2\ T_{obs}$ represents the changes $pCO_{2\ obs}$ induced by temperature fluctuations, and $pCO_{2\ mean}$ is the mean $pCO_{2\ obs}$ over the studied period. The changes related to temperature were estimated as following:

$$(\Delta pCO_2)_{temp} = (pCO_2\ T_{obs})_{max} - (pCO_2\ T_{obs})_{min} \tag{8}$$

The relative importance of temperature (T) and biology (B) effects on $pCO_{2,\ sea}$ is expressed in terms of the following ratio:

$$T/B = (\Delta pCO_2)_{temp}/(\Delta pCO_2)_{bio} \quad (9)$$

2.6. Statistical analyses

A general linear model (seasons and sites were fixed effects) was used to test for significance for nutrients (DIN and DIP) and seagrass biological parameters (seagrass density and leaf biomass). One-way analysis of variance (ANOVA) was used to determine the statistical significance of T/B and $F_{CO_2,day}$ among the three sampling sites, with the seasonal data as replicates. Seasonal differences of T/B and $F_{CO_2,day}$ (absolute value) with site data as replicates were analyzed by one-way ANOVA. Tukey post hoc tests were applied to identify the significantly different components of the above parameters. Pearson correlation analysis was determined between the T/B and natural logarithm transformed seagrass density and leaf biomass. The minimum significance level set for statistical difference was $p < 0.05$. All statistical analyses were performed with IBM SPSS Statistics 23.0 software (IBM SPSS Statistics 19, IBM Corporation, Somers, NY) and Microsoft Office Excel 2007 (Microsoft Corporation, Redmond, WA).

3. Results and discussion

3.1. Variations of nutrients and seagrass biological traits

The average DIN and DIP ranged from 1.55 to 28.07 μmol L^{-1}, and 0.13 to 2.39 μmol L^{-1}, respectively (Fig. S1). DIN and DIP concentrations were significantly influenced by sampling site, season and their interaction (Table 1, $p < 0.001$). Average DIN and DIP in Xincun were ~2.5 and ~3-fold higher than Li'an and Tanmen, respectively, with a trend of Xincun > Li'an > Tanmen (Fig. S1b, d). This was ascribed to different human activities that pollute these three seagrass meadows, and is consistent with our previous study (Liu et al., 2020). Further, the DIN and DIP of the three sites in autumn were significantly higher than other seasons (Fig. S1a, c).

With exception of *E. acoroides* density, other seagrass traits were significantly different among the four seasons (Table 1, *T. hemprichii* density: $p = 0.009$; *T. hemprichii* and *E. acoroides* leaf biomass: $p < 0.001$). Maximum *T. hemprichii* density and leaf biomass, and *E. acoroides* leaf biomass were presented in summer (Figs. 2a, 3a, c), which may be associated with higher temperature and irradiation intensity in summer (Kenyon et al., 1997; Lin and Shao, 1998). Lower waters at spring tide that occurred during the daytime in autumn (2021 Tide Tables) caused a significant loss of seagrass density and leaf biomass, due to the desiccation effect (Figs. 2a, 3a, c) (Erftemeijer and Herman, 1994). The highest seawater DIN and DIP observed in autumn supported our hypothesis as well, i.e. seagrass leaf biomass senescence and loss can release abundant inorganic nutrients during leaching period. *E. acoroides* density tended to be similar among the four seasons (Fig. 2c; Table 1, $p = 0.120$), although *E. acoroides* leaf biomass showed marked decreased in autumn. This finding was consistent with a previous study that reported *E. acoroides* as more desiccation-resistant than *T. hemprichii* (Jiang et al., 2014). Overall, the annual total seagrass leaf biomass values observed a trend of summer > winter ≈ spring > autumn (Fig. 3a, c).

The average densities of *T. hemprichii* and *E. acoroides* in Tanmen, Li'an and Xincun were 424.25 ± 50.04 and 137.25 ± 12.42 shoots m^{-2}, 240.00 ± 21.23 and 112.00 ± 9.66 shoots m^{-2}, and 275.00 ± 17.54 and 163.00 ± 5.97 shoots m^{-2}, respectively (Fig. 2). For seagrass leaf biomass, the average *T. hemprichii* leaf biomass was 53.91 ± 12.98, 30.54 ± 8.11 and 31.15 ± 8.97 g m^{-2} in Tanmen, Li'an and Xincun, respectively, while the average *E. acoroides* leaf biomass was 100.82 ± 22.37, 93.09 ± 27.75 and 129.69 ± 29.31 g m^{-2}, respectively (Fig. 3). Similar to the nutrient loading levels, the *T. hemprichii* density and leaf biomass in Tanmen were significantly higher than that in Li'an and Xincun (Figs. 2b, 3b; Table 1, $p < 0.001$). In contrast to *T. hemprichii*, the highest *E. acoroides* density and leaf biomass were observed in Li'an (Figs. 2d, 3d), and showed significant differences among the three sites (Table 1, $p < 0.001$). High nutrient loading led to much higher biomass of macroalgae and epiphytes in Li'an and Xincun than in Tanmen (Cui et al., 2021; Liu et al., 2020), which consequently decreased the density and biomass of the smaller seagrass *T. hemprichii* by inducing shading. The taller *E. acoroides* can lift its leaves much closer to the water surface, and has a high nutrient demand (Agawin et al., 1996; Vermaat et al., 2017), which should be responsible for the highest *E. acoroides* density and biomass in a relatively high nutrient loading seagrass meadow.

Table 1
Statistical analysis of the effects of the site and season on nutrients and seagrass biological parameters using general linear model (site and season as the fixed effects). Values reported are *F*-statistics.

Parameters	Site	Season	Site×Season
DIN	85.366***	104.393***	34.084***
DIP	81.827***	23.629***	14.078***
T. hemprichii density	27.325***	4.506**	2.996*
E. acoroides density	17.004***	1.837	1.585
T. hemprichii leaf biomass	38.839***	60.050***	4.410**
E. acoroides leaf biomass	19.978***	108.899***	2.716*

* $0.01 < p \leq 0.05$.
** $0.001 < p \leq 0.01$.
*** $p \leq 0.001$.

3.2. Variations of hydrography and wind velocity

Hydrographic and wind speed parameters were observed for continuous 24 h among the three seagrass meadows at each season. There was no diurnal variability of salinity, with the majority fluctuations of salinity <0.5. The average lowest and highest salinity was observed in autumn (32.31) and summer (33.87), and the annual average salinity was 32.91, 33.57 and 33.62 in Tanmen, Li'an and Xincun, respectively. Since there is no river input influencing these seagrass meadows, the little variations of salinity among the three seagrass meadows in different seasons should be mainly due to rainfall or typhoon. Diurnal oscillation of temperature was <2.5 °C during the study period among the three seagrass meadows, but not during the in summer in Tanmen (~6 °C) (Fig. S2). Consistent with our previous study (Liu et al., 2020), diurnal average temperatures were similar in spring, summer and autumn among the three seagrass meadows. Additionally, average temperatures in spring, summer and autumn were 29.22, 31.55 and 25.50 °C, respectively (Fig. S2b, c, d). However, the average winter temperature in Tanmen (18.26 °C) was ~5 °C less than Li'an and Xincun (23.56 °C) (Fig. S2a). This should be due to cold and rainy weather in Tanmen during the sampling period in winter, while the weather in Li'an and Xincun was relatively warm and sunny during the winter sampling period.

The μ_{10} is the wind velocity at a height of 10 m above sea surface, which was calculated from wind velocity at 1 m in height (Sutton et al., 2017). The μ_{10} exhibited a diurnal oscillation, as shown in Fig. S3. The μ_{10} generally started to increase from 06:00, approached the peak during the afternoon (15:00– 18:00) and then declined until around 0:00–3:00 (Fig. S3). Average μ_{10} was 3.56 ± 0.39 m s^{-1} over the whole sampling period and ranged between 0 and 9.47 m s^{-1} (Fig. S3). Annual average μ_{10} was 4.33, 3.38 and 2.96 m s^{-1} in Tanmen, Li'an and Xincun seagrass meadows, respectively. Further, the average μ_{10} in autumn was 1.5–1.7 fold higher than other seasons (Fig. S3).

3.3. Variations of pCO_2 and its affecting factors

Seawater pCO_2 ($pCO_{2,sea}$) diel fluctuations ranged from 164 to 692 μatm, 270 to 497 μatm, and 217 to 576 μatm during the sampling periods in Tanmen, Li'an and Xincin seagrass meadows, respectively

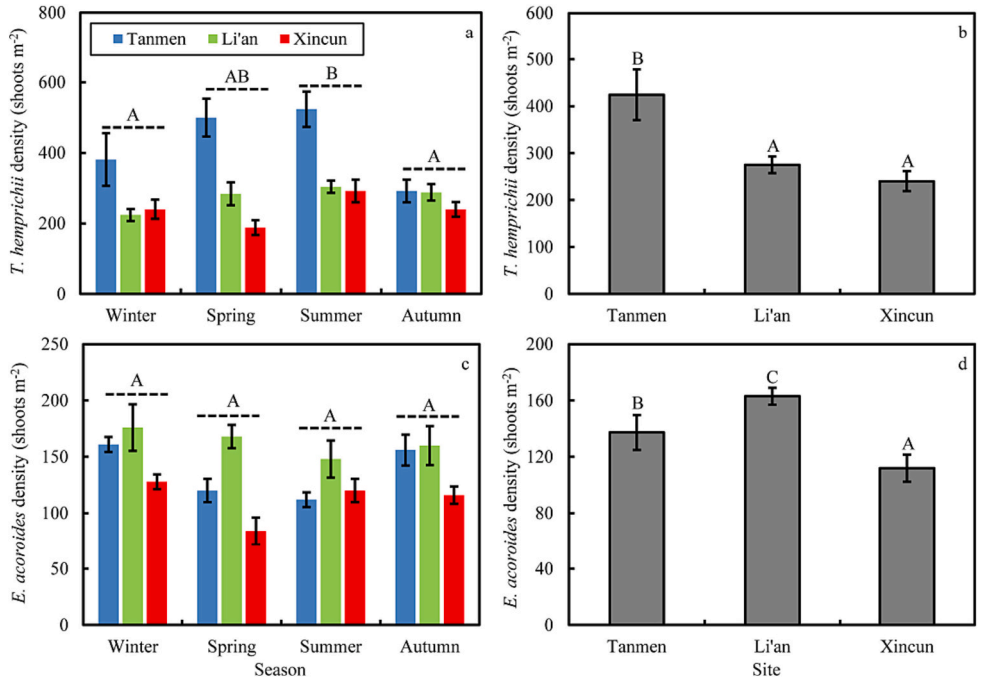

Fig. 2. *T. hemprichii* density in different seasons (a) and different sites (b), and *E. acoroides* density in different seasons (c) and different sites (d). The different capital letters over the bars indicate significant differences among the four seasons or the three sites (Tukey post hoc test, $p < 0.05$).

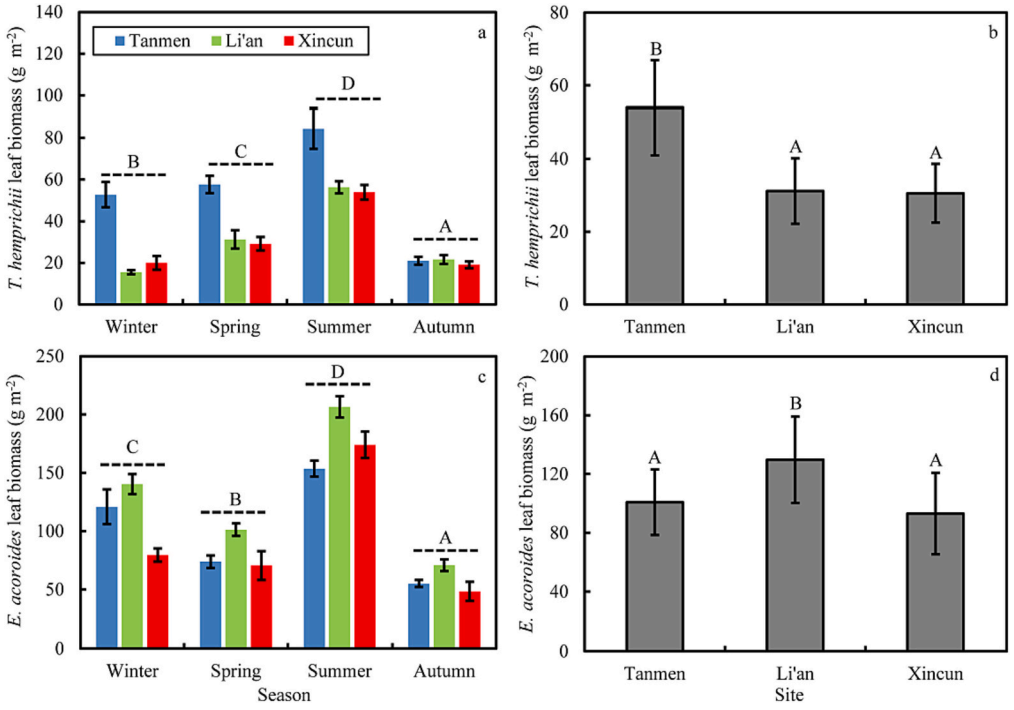

Fig. 3. *T. hemprichii* leaf biomass in different seasons (a) and different sites (b), and *E. acoroides* leaf biomass in different seasons (c) and different sites (d). The different capital letters over the bars indicate significant differences among the four seasons or the three sites (Tukey post hoc test, $p < 0.05$).

(Fig. 4). These values are consistent with several other studies where time series of $pCO_{2,\ sea}$ in seagrass meadows have been recorded. For example, Yates et al. (2007) reported that $pCO_{2,\ sea}$ ranged from 260 to 497 μatm over a few diel cycles in *Thalassia testudinum* dominated meadows of subtropical Florida Bay. In a temperate *Zostera marina* meadow of the South Bay, $pCO_{2,\ sea}$ showed a range from 193 to 859 μatm during the several diel variation observations (Berg et al., 2019). Diurnal oscillation of $pCO_{2,\ sea}$ was mainly expected to be dependent on the combined influence of temperature and biological processes (Akhand et al., 2021; Chien et al., 2018; Urbini et al., 2020). The relative importance of biology and temperature effects on $pCO_{2,\ sea}$ is expressed by the T/B (Fig. 5). It noted that the computational formula of biology and temperature effects on $pCO_{2,\ sea}$ was derived from the open ocean (Takahashi et al., 2002). In contrast to the open sea, coastal oceans have more dynamic and complex biogeochemical and physical processes, which may have different effects on $pCO_{2,\ sea}$ when compared to the

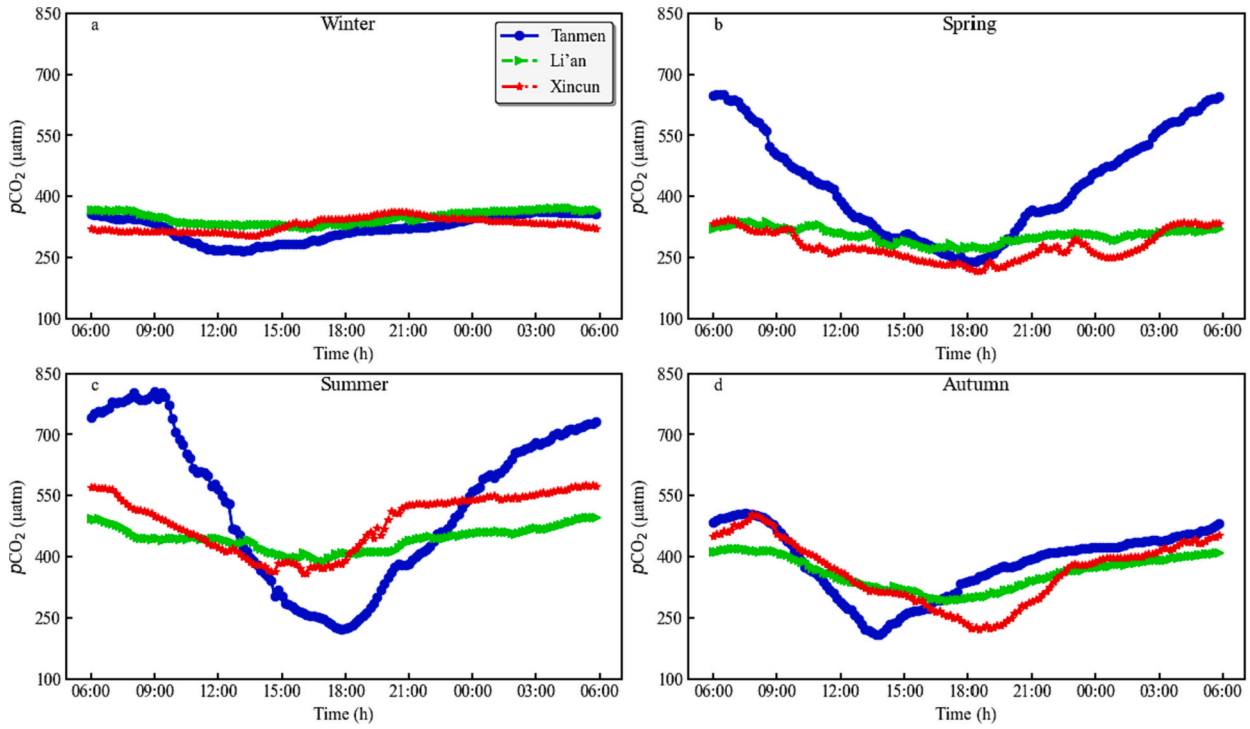

Fig. 4. Winter (a), spring (b), summer (c) and autumn (d) temporal (diurnal) variability of $pCO_{2,\ sea}$ in Tanmen, Li'an and Xincun seagrass meadows.

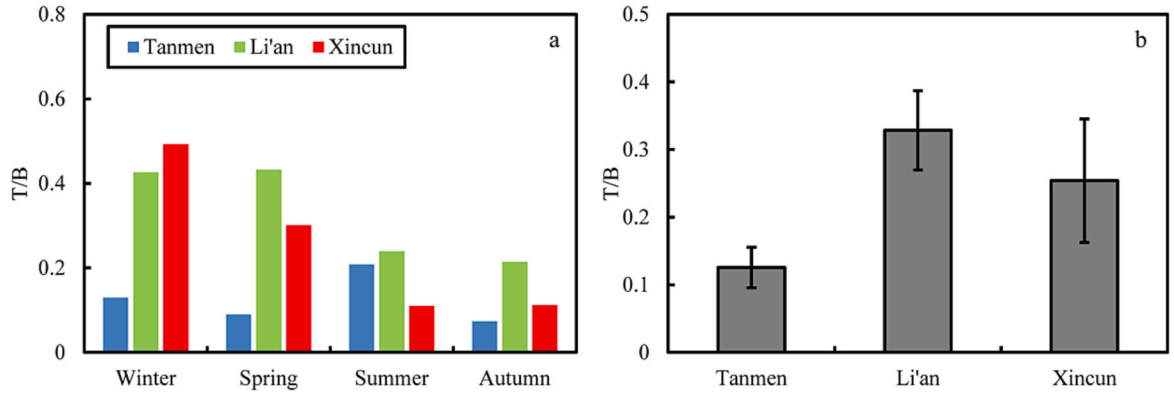

Fig. 5. Thermic/biological $pCO_{2,\ sea}$ ratio (T/B) in different seasons (a) and different sites (b). No significant differences of T/B were observed in different seasons and different sites (Tukey post hoc test, $p < 0.05$).

$pCO_{2,\ sea}$ in open ocean waters. However, the computational formula has been widely applied in coastal ecosystems, including seagrass ecosystems, where there are no obvious effects of horizontal (upwelling) and vertical (river input) mixing (Ávila-López et al., 2017; Chen and Hu, 2019; De Carlo et al., 2013; Wimart-Rousseau et al., 2020). Therefore, we can roughly estimate the temperature and biology effects on $pCO_{2,\ sea}$ in this study. All the ratios of the three seagrass meadows at four seasons were <1 (Fig. 5a), indicating the biological effect exceeds the temperature effects during each sampling period of the three sites (Ávila-López et al., 2017; Urbini et al., 2020). Diel $pCO_{2,\ sea}$ variations induced by biological effects were expected to be dependent on the photosynthesis and community respiration processes that associate with diurnal solar insulation (Chien et al., 2018). Additionally, atmospheric pCO_2 ($pCO_{2,\ atm}$) was also recorded in this study. The differences of $pCO_{2,\ atm}$ among the three seagrass meadows were <15 μatm at each season, and the diurnal variations of $pCO_{2,\ atm}$ were generally <10 μatm. The average $pCO_{2,\ atm}$ was 430.67, 391.13, 412.33 and 400.99 μatm in winter, spring, summer and autumn, respectively. The diurnal oscillation of ΔpCO_2 ($pCO_{2,\ sea}$ - $pCO_{2,\ atm}$, μatm) was calculated and presented in Fig. S4. ΔpCO_2 values were generally negative from late morning or noon to before midnight, that increased from after midnight to early morning or noon (Fig. S4). This indicated a net uptake of atmospheric CO_2 from the late morning or noon to before midnight, and a CO_2 sink or CO_2 source after midnight to early morning or noon (Chien et al., 2018; De Carlo et al., 2013).

The seasonal mean variation range of $pCO_{2,\ sea}$ on the Li'an and Xincun seagrass meadows was similar, ~300–480 μatm, compared to ~320–527 μatm in the Tanmen seagrass meadow (Fig. 4). The average $pCO_{2,\ sea}$ of the three seagrass meadows in different seasons displayed a clear trend with values increasing from spring, reaching maximum in summer and then decreasing after summer, which was similar to a previous study showing seasonal $pCO_{2,\ sea}$ variations in *Zostera marina* seagrass meadows of San Quintín Bay (Ávila-López et al., 2017). The highest mean $pCO_{2,\ sea}$ was observed in summer and is likely driven by higher temperatures and high (~double) seagrass biomass compared to winter and spring. There are several potential reasons for an increase in

$pCO_{2,\ sea}$ in summer. Firstly, warm summer temperatures decreased CO_2 solubility in seawater (Van Dam et al., 2021b). Secondly, the summer average temperature in summer at the three sites was ~31 °C, which is far beyond the optimal photosynthesis temperature of *T. hemprichii* and *E. acoroides* (27 °C), and might have decreased the seagrass photosynthetic efficiency (Agawin et al., 2001). Third, exposure to high water temperatures promotes respiration of the seagrass relative to photosynthesis (Berg et al., 2019). Additionally, much higher $pCO_{2,\ sea}$ in autumn than in spring and winter might be attributed to abundant seagrass leaf detritus decomposition, leading to high organic carbon metabolism. These reasons can also explain the relatively lower T/B in summer and autumn than in spring and summer, despite no significant difference of the T/B among the four seasons ($F = 1.424$, $p = 0.306$; Fig. 5a). This indicates stronger biological effects in $pCO_{2,\ sea}$ changes in summer and autumn.

Mean annual $pCO_{2,\ sea}$ values were 416, 364 and 365 μatm in Tanmen, Li'an and Xincin seagrass meadows, respectively (Fig. 4). Winter and autumn mean $pCO_{2,\ sea}$ at three sites were similar (~320–350 μatm and ~ 360–380 μatm in winter and autumn, respectively) (Fig. 4a, d), but spring and summer mean $pCO_{2,\ sea}$ were markedly higher on the Tanmen compared to the Li'an and Xincun seagrass meadows (Fig. 4b, c). Tanmen is an open-water harbor, with faster currents and larger waves compared to the slower flow of the shallow waters of Xincun and Li'an (Deng et al., 2021). We hypothesized that turbulence might result in increasing oxygen diffusion at the sediment surface of Tanmen, which consequently enhanced benthic respiration during particularly high temperatures in spring and summer (Bahlmann et al., 2015). The mean sediment redox potential at the Tanmen seagrass meadow (−103 mv) was much higher than Li'an and Xincun seagrass meadows (−205 and −226 mv, respectively) (unpublished data), also supporting our hypothesis. Further, although T/B was not significantly different among the three sites ($F = 2.490$, $p = 0.138$), the annual mean T/B in Tanmen was 0.13, which was less than that in Li'an (0.33) and Xincun (0.25) (Fig. 5b). This indicates biological effects on $pCO_{2,\ sea}$ variations contributed more in Tanmen than Li'an and Xincun. As previously mentioned, Tanmen had the highest *T. hemprichii* density and leaf biomass but not *E. acoroides* density and leaf biomass (Figs. 2 and 3). Previous studies have reported that approximately 60 % inorganic carbon uptake by *E. acoroides* was HCO_3^- (Björk et al., 1997), while *T. hemprichii* mainly uptake CO_2 in seawater (Jiang et al., 2010). We assumed that $pCO_{2,\ sea}$ was mainly mediated by the *T. hemprichii* community, but not the *E. acoroides* community. Additionally, correlation analysis showed that there were stronger correlations between T/B and *T. hemprichii* density and leaf biomass than between T/B and *E. acoroides* density and leaf biomass (Fig. S5), further supporting our assumption.

3.4. Air-sea CO_2 flux and ecological implications

Air-sea CO_2 flux is a function of gas transfer velocity, solubility coefficients and ΔpCO_2, which was closely associated with seawater temperature, salinity and μ_{10} (Li et al., 2020; Van Dam et al., 2021b). The instantaneous (minutes) air-sea CO_2 fluxes (F_{CO_2}) were shown in Fig. 6, which exhibited a U-shape diurnal variability from 6 a.m. to 6 a.m. the next day. During the diurnal observation, all F_{CO_2} values were negative in winter, while most instantaneous air-sea CO_2 fluxes were positive in summer (Fig. 6a, c). In spring and autumn, most F_{CO_2} values were negative (Fig. 6b, d). The daily air-sea CO_2 flux ($F_{CO_2,day}$) values were calculated by summing the instantaneous F_{CO_2} values. No significant differences were observed for the absolute values of $F_{CO_2,day}$ among the four seasons ($F = 1.970$, $p = 0.197$). Except for during summer, all $F_{CO_2,day}$ values were negative, indicating a net uptake of CO_2 in the three seagrass meadows during winter, spring, and autumn, but outgassing of CO_2 during summer (Fig. 7a). This contrasts with temperate *Zostera marina* meadows, which have been reported as a CO_2 sink from May to August, and a CO_2 source from September to November (Tokoro et al., 2014). The tropical seagrasses *T. hemprichii* and *E. acoroides* grow all-year round (Rollón, 1998), but temperate *Z. marina* grows rapidly in the spring and summer and then mostly decays during autumn and winter (Zhou et al., 2015). This might partially explain the different

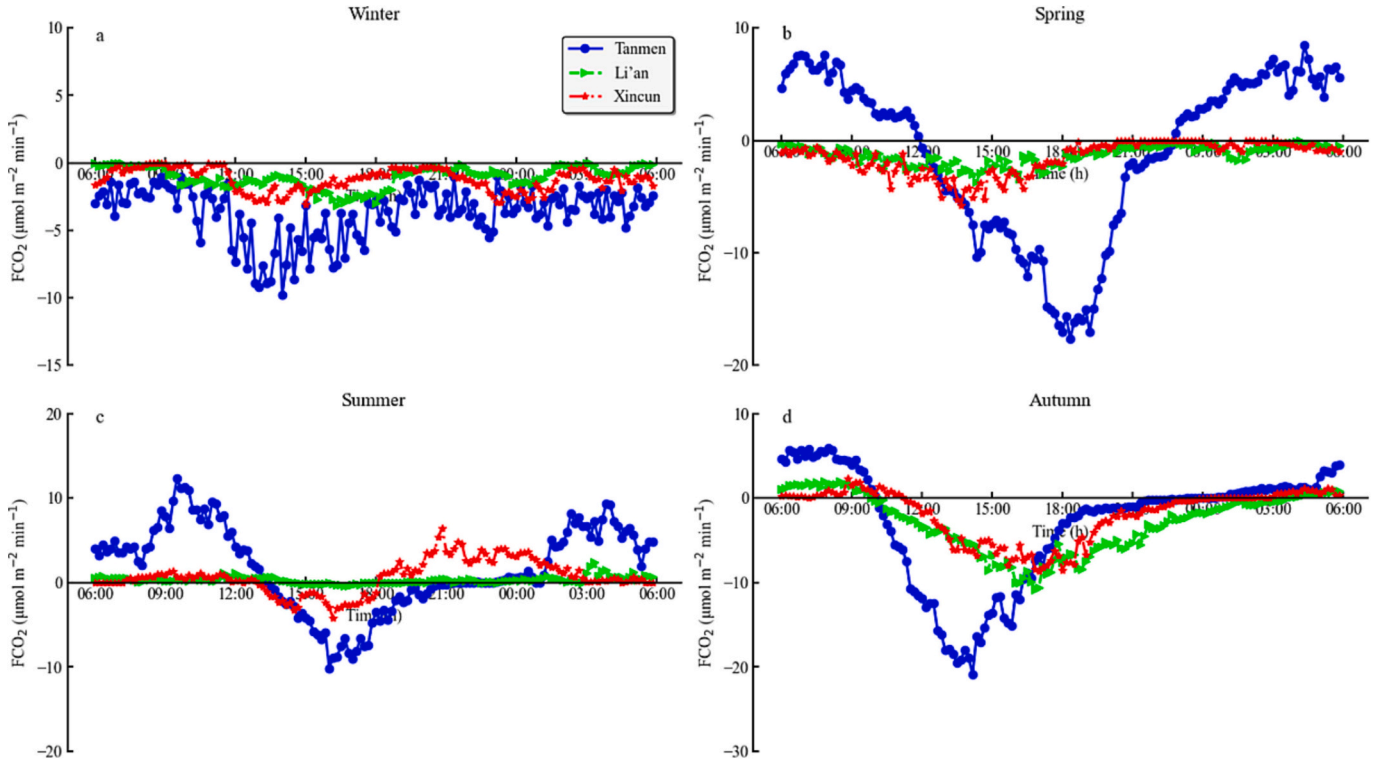

Fig. 6. Winter (a), spring (b), summer (c) and autumn (d) temporal (diurnal) variability of air-sea CO_2 flux in Tanmen, Li'an and Xincun seagrass meadows. Positive F_{CO_2} values indicate gas fluxes from water to the atmosphere, while negative values indicate fluxes from the atmosphere to water.

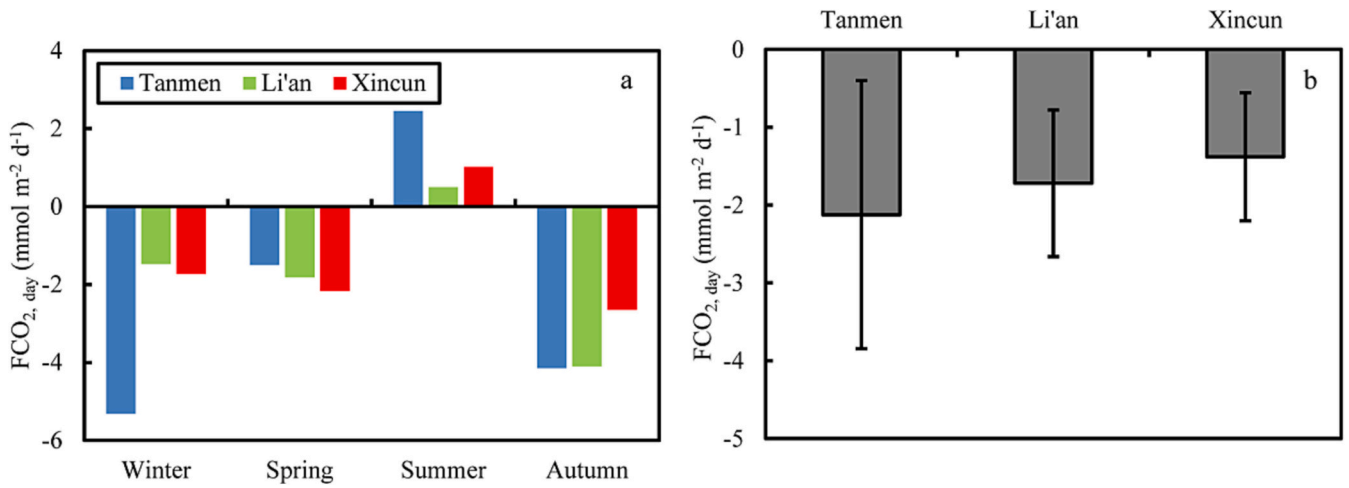

Fig. 7. Diurnal air-sea CO_2 fluxes ($F_{CO_{2,day}}$) in different seasons (a) and different sites (b). No significant differences of T/B were observed in different seasons and different sites (Tukey post hoc test, $p < 0.05$). Positive $F_{CO_{2,day}}$ values indicate gas fluxes from water to the atmosphere, while negative values indicate fluxes from the atmosphere to water.

seasonal patterns of $F_{CO_{2,day}}$. Additionally, although the ΔpCO_2 was more negative in winter than in autumn, average $F_{CO_{2,day}}$ of the three sites in autumn (-3.63 ± 0.76 mmol m^{-2} d^{-1}) was more negative than that in winter (-2.84 ± 0.60 mmol m^{-2} d^{-1}) (Fig. 7a). The μ_{10} was higher in autumn than in other seasons, which should be responsible for the greater uptake of atmospheric CO_2 in autumn (Wanninkhof and Triñanes, 2017). Average $F_{CO_{2,day}}$ at each sampling site was calculated based on the values of the four seasons (Fig. 7b). Although there was no significant difference in average $F_{CO_{2,day}}$ among the three sites ($F = 0.092$, $p = 0.913$), the average $F_{CO_{2,day}}$ in Tanmen (-2.12 ± 0.45 mmol m^{-2} d^{-1}) was 23 % and 54 % more negative than Li'an and Xincun seagrass meadows, respectively (Fig. 7b). Relatively lower temperatures (mainly in winter) and higher wind velocity in Tanmen contributed to the net uptake of atmospheric CO_2. Further, as mentioned above, the biological effect (especially the seagrass *T. hemprichii*) was the driving force for $pCO_{2,\ sea}$ control in our study seagrass meadows, and the high *T. hemprichii* density and biomass in Tanmen is also likely responsible for the higher CO_2 flux from atmosphere to sea.

The mean annual fluxes (based on average air-sea CO_2 fluxes ($F_{CO_{2,year}}$) over the four seasons) were -0.78 ± 0.16, -0.63 ± 0.13 and -0.50 ± 0.11 mol m^{-2} yr^{-1} at Tanmen, Li'an and Xincun seagrass meadows, respectively. The estimated $F_{CO_{2,year}}$ in seagrass meadows of Hainan Island were in the range of global values (Table 2). Global $F_{CO_{2,year}}$ of seagrass meadows exhibited significant spatial heterogeneity, with some seagrass meadows even acting as CO_2 sources. However, the absolute values of $F_{CO_{2,year}}$ measured by the eddy covariance method were shown to be higher than that measured by the bulk formula method (Table 2). Erkkilä et al. (2018) reported similar results, and explained that the estimation error of gas transfer velocity (k) mainly resulted in lower air-sea CO_2 flux of the bulk formula method than the eddy covariance method. Moreover, the bulk formula method was always applied in the air-sea CO_2 flux of monthly or seasonal surveys (Ávila-López et al., 2017; Maher and Eyre, 2012), in contrast with the continuous and automatic monitoring of the eddy covariance method (Van Dam et al., 2021a), which could also be responsible for the differences between the two methods. In this study we only conducted four seasons of surveys in three seagrass meadows using the bulk formula method, which might underestimate the net uptake CO_2 potential in tropical seagrass meadows. As a matter for future research, we recommend continuously monitoring the tropical seagrass meadows air-sea CO_2 flux using the eddy covariance method. Such research will help to determine accurate estimates of air-sea CO_2 flux, with important implications for carbon budget accounting in seagrass meadows.

Table 2
Comparison of annual air-sea CO_2 flux of global seagrass meadows.

Study area	Seagrass species	Method	Annual air-sea CO_2 flux	References
San Quintín Bay, Baja California, Mexico	*Zostera marina*	Bulk formula method	1.20 mol m^{-2} yr^{-1}	(Ávila-López et al., 2017)
Bay of Revellata, North-Western Corsisa, France	*Posidonia oceanica*	Bulk formula method	−0.7 mol m^{-2} yr^{-1}	(Champenois and Borges, 2021)
Hastings River estuary, southeast coast of Australia	*Zostera capricorni*, *Halophila ovalis*	Bulk formula method	−0.4 ± 0.6 mol m^{-2} yr^{-1}	(Maher and Eyre, 2012)
Camden Haven, southeast coast of Australia	*Z. capricorni*, *H. ovalis*, *Ruppia megacarpa*	Bulk formula method	−1.8 ± 0.6 mol m^{-2} yr^{-1}	(Maher and Eyre, 2012)
Wallis Lake, southeast coast of Australia	*Z. capricorni*, *H. ovalis*, *R. megacarpa*, *Posidonia australis*	Bulk formula method	−2.0 ± 0.9 mol m^{-2} yr^{-1}	(Maher and Eyre, 2012)
Estero El Soldado, Mexico	*Z. marina*	Eddy covariance method	−4.1 mol m^{-2} yr^{-1}	(Van Dam et al., 2021a)
Furen lagoon, Japan	*Z. marina*	Eddy covariance method	−32.8 mol m^{-2} yr^{-1}	(Van Dam et al., 2021a)
Bob Allen Keys, America	*Thalassia testudinum*	Eddy covariance method	1.80 mol m^{-2} yr^{-1}	(Van Dam et al., 2021a)
Tanmen, Hainan Island, China	*Thalassia hemprichii*, *Enhalus acoroides*	Bulk formula method	−0.78 ± 0.16 mol m^{-2} yr^{-1}	This study
Li'an, Hainan Island, China	*T. hemprichii*, *E. acoroides*	Bulk formula method	−0.63 ± 0.13 mol m^{-2} yr^{-1}	This study
Xincun, Hainan Island, China	*T. hemprichii*, *E. acoroides*	Bulk formula method	−0.50 ± 0.11 mol m^{-2} yr^{-1}	This study

Average $F_{CO_2,year}$ of the three seagrass meadows was −0.64 ± 0.13 mol m^{-2} yr^{-1}. According to our previous field survey, the entire area of seagrass meadows in Hainan Island was 5527.73 ha. >90 % of the area of seagrass meadows distributed along the eastern coastline of Hainan Island were composed by seagrass of *T. hemprichii* and *E. acoroides* (Huang et al., 2006). These three study sites were the representative seagrass meadows along the eastern coastal of Hainan Island. Therefore, if we assume that all the seagrass meadows have similar $F_{CO_2,year}$, then the annual atmospheric CO_2 uptake in seagrass meadows of Hainan Island can be roughly estimated as 1544.45 ± 316.19 t CO_2 yr^{-1}. This rate is equivalent to the annual emissions of 164,000 tourists in Hainan Island for the wholesale, retail, accommodation and catering industries (Wu et al., 2015). Further, we have shown that Li'an and Xincun were 23–54 % lower $F_{CO_2,year}$ than Tanmen. As discussed above, high nutrient loading has led to seagrass decline, and is the likely cause for the observed decrease in the net uptake of atmospheric CO_2, when compared with a relatively low nutrient loading seagrass meadow. While our estimate is based on only three seagrass meadows from one region of the world and should therefore be considered a 'back of the envelope' estimate, it certainly suggests that air-sea CO_2 flux potential is affected by nutrient loading, which could be of global significance given how widespread nutrient pollution has become.

Despite this, empirical evidence on the effect of nutrient loading associated with seagrass biomass changes on air-sea flux is rare. For future studies, we recommend using net community metabolism and $pCO_{2,sea}$ to evaluate potential relationships in seagrass biomass and air-sea CO_2 flux among seagrass meadows under different nutrient loads. Lee et al. (2007) reported the DIN and DIP concentrations of global subtropical/tropical seagrass meadows seawater were generally <4 and 0.5 μmol L^{-1}, respectively, with the exception of areas characterized by mesotrophic, eutrophic and hypereutrophic sites. In compare with this study, the nutrients in Tanmen seagrass meadow were similar to the relative low nutrient loading levels of global subtropical/tropical seagrass meadows, but not in the Xincun and Li'an seagrass meadows. Nutrient loading induced seagrass decline could consequently decrease the potential of uptake of atmospheric CO_2. Therefore, we suggest reducing nutrient discharge in seagrass meadows (controlling the nutrient concentrations to similar or less than those in Tanmen), and the restoration of degraded seagrass meadows to help promote net CO_2 uptake, which could have important implications for global carbon neutrality.

4. Conclusion

This study suggests that the tropical seagrass meadows of Hainan Island in the South China Sea can be a significant contributor to atmospheric CO_2 uptake. Over the whole sampling period, the air-sea CO_2 fluxes of the three seagrass meadows ranged from −0.78 to −0.50 mol m^{-2} yr^{-1}, with the temperature, wind velocity and status of seagrass growth as the main driving factors. Further, high nutrient loadings caused seagrass decline and reduced annual CO_2 uptake potential by 23–54 %. We recommend reducing nutrient discharge and restoring degraded seagrass meadows to promote net atmospheric CO_2 uptake. Due to limited information on the effects of nutrient loading on air-sea CO_2 flux in seagrass meadows, we recommend further research into the relationships between net seagrass community metabolism and $pCO_{2,sea}$, and their response to nutrient loading.

CRediT authorship contribution statement

Songlin Liu: Conceptualization, Methodology, Investigation, Writing – original draft. **Jiening Liang:** Resources, Data curation, Formal analysis. **Zhijian Jiang:** Investigation, Formal analysis. **Jinlong Li:** Investigation, Validation. **Yunchao Wu:** Formal analysis, Software. **Yang Fang:** Investigation, Data curation. **Yuzheng Ren:** Resources, Data curation. **Xia Zhang:** Investigation, Software. **Xiaoping Huang:** Writing – review & editing, Funding acquisition. **Peter I. Macreadie:** Writing – review & editing.

Declaration of competing interest

The authors declare that they have no known competing financial interests or personal relationships that could have appeared to influence the work reported in this paper.

Data availability

Data will be made available on request.

Acknowledgements

This work was supported by the National Natural Science Foundation of China (U1901221, 42176155), the Youth Innovation Promotion Association CAS (2023359), National Key Research and Development Program of China (2022YFF0802201), the Key Research and Development Project of Hainan Province (ZDYF2021SHFZ254), and the Science and Technology Planning Project of Guangdong Province, China (2023B1212060047). PM thanks support from an Australian Research Council Discovery Grant (DP200100575).

Appendix A. Supplementary data

Supplementary data to this article can be found online at https://doi.org/10.1016/j.scitotenv.2023.168684.

References

Agawin, N.S., Duarte, C.M., Fortes, M.D., 1996. Nutrient limitation of Philippine seagrasses (Cape Bolinao, NW Philippines): *in situ* experimental evidence. Mar. Ecol. Prog. Ser. 138, 233–243.
Agawin, N.S.R., Duarte, C.M., Fortes, M.D., Uri, J.S., Vermaat, J.E., 2001. Temporal changes in the abundance, leaf growth and photosynthesis of three co-occurring Philippine seagrasses. J. Exp. Mar. Biol. Ecol. 260, 217–239.
Akhand, A., Watanabe, K., Chanda, A., Tokoro, T., Chakraborty, K., Moki, H., et al., 2021. Lateral carbon fluxes and CO_2 evasion from a subtropical mangrove-seagrass-coral continuum. Sci. Total Environ. 752, 142190.
Ávila-López, M.C., Hernández-Ayón, J.M., Camacho-Ibar, V.F., Bermúdez, A.F., Mejía-Trejo, A., Pacheco-Ruiz, I., et al., 2017. Air–water CO_2 fluxes and net ecosystem production changes in a Baja California coastal lagoon during the anomalous North Pacific warm condition. Estuar. Coasts 40, 792–806.
Bahlmann, E., Weinberg, I., Lavrič, J., Eckhardt, T., Michaelis, W., Santos, R., et al., 2015. Tidal controls on trace gas dynamics in a seagrass meadow of the Ria Formosa lagoon (southern Portugal). Biogeosciences 12, 1683–1696.
Banerjee, K., Paneerselvam, A., Ramachandran, P., Ganguly, D., Singh, G., Ramesh, R., 2018. Seagrass and macrophyte mediated CO_2 and CH_4 dynamics in shallow coastal waters. PLoS One 13, e0203922.
Barrón, C., Duarte, C.M., Frankignoulle, M., Borges, A.V., 2006. Organic carbon metabolism and carbonate dynamics in a Mediterranean seagrass (*Posidonia oceanica*) meadow. Estuar. Coasts 29, 417–426.
Bauer, J.E., Cai, W.J., Raymond, P.A., Bianchi, T.S., Hopkinson, C.S., Regnier, P.A., 2013. The changing carbon cycle of the coastal ocean. Nature 504, 61–70.
Berg, P., Delgard, M.L., Polsenaere, P., McGlathery, K.J., Doney, S.C., Berger, A.C., 2019. Dynamics of benthic metabolism, O_2, and pCO_2 in a temperate seagrass meadow. Limnol. Oceanogr. 64, 2586–2604.
Björk, M., Weil, A., Semesi, S., Beer, S., 1997. Photosynthetic utilisation of inorganic carbon by seagrasses from Zanzibar, East Africa. Mar. Biol. 129, 363–366.
Champenois, W., Borges, A.V., 2021. Net community metabolism of a *Posidonia oceanica* meadow. Limnol. Oceanogr. 66, 2126–2140.
Chen, S., Hu, C., 2019. Environmental controls of surface water pCO_2 in different coastal environments: observations from marine buoys. Cont. Shelf Res. 183, 73–86.
Chien, H., Zhong, Y.Z., Yang, K.H., Cheng, H.Y., 2018. Diurnal variability of CO_2 flux at coastal zone of Taiwan based on eddy covariance observation. Cont. Shelf Res. 162, 27–38.
Cui, L., Jiang, Z., Huang, X., Chen, Q., Wu, Y., Liu, S., et al., 2021. Eutrophication reduces seagrass contribution to coastal food webs. Ecosphere 12, e03626.
De Carlo, E.H., Mousseau, L., Passafiume, O., Drupp, P.S., Gattuso, J.P., 2013. Carbonate chemistry and air–sea CO_2 flux in a NW Mediterranean bay over a four-year period: 2007–2011. Aquat. Geochem. 19, 399–442.
Deng, Y., Liu, S., Feng, J., Wu, Y., Mao, C., 2021. What drives putative bacterial pathogens removal within seagrass meadows? Mar. Pollut. Bull. 166, 112229.

Duarte, C.M., Kennedy, H., Marbà, N., Hendriks, I., 2013. Assessing the capacity of seagrass meadows for carbon burial: current limitations and future strategies. Ocean Coast. Manag. 83, 32–38.
Erftemeijer, P.L., Herman, P.M., 1994. Seasonal changes in environmental variables, biomass, production and nutrient contents in two contrasting tropical intertidal seagrass beds in South Sulawesi, Indonesia. Oecologia 99, 45–59.
Erkkilä, K.M., Ojala, A., Bastviken, D., Biermann, T., Heiskanen, J.J., Lindroth, A., et al., 2018. Methane and carbon dioxide fluxes over a lake: comparison between eddy covariance, floating chambers and boundary layer method. Biogeosciences 15, 429–445.
Fu, C., Li, Y., Zeng, L., Zhang, H., Tu, C., Zhou, Q., et al., 2021. Stocks and losses of soil organic carbon from Chinese vegetated coastal habitats. Glob. Chang. Biol. 27, 202–214.
Gazeau, F., Duarte, C.M., Gattuso, J.P., Barrón, C., Navarro, N., Ruiz, S., et al., 2005. Whole-system metabolism and CO_2 fluxes in a Mediterranean Bay dominated by seagrass beds (Palma Bay, NW Mediterranean). Biogeosciences 2, 43–60.
Huang, X., Huang, L., Li, Y., Xu, Z., Fong, C.W., Huang, D., et al., 2006. Main seagrass beds and threats to their habitats in the coastal sea of South China. Chin. Sci. Bull. 51 (Suppl. 2), 136–142.
Huang, Y., Xiao, X., Xu, C., Perianen, Y.D., Hu, J., Holmer, M., 2020. Seagrass beds acting as a trap of microplastics - emerging hotspot in the coastal region? Environ. Pollut. 257, 113450.
Jiang, L.Q., Cai, W.J., Wang, Y., 2008. A comparative study of carbon dioxide degassing in river-and marine-dominated estuaries. Limnol. Oceanogr. 53, 2603–2615.
Jiang, Z.J., Huang, X.P., Zhang, J.P., 2010. Effects of CO_2 enrichment on photosynthesis, growth, and biochemical composition of seagrass *Thalassia hemprichii* (Ehrenb.) Aschers. J. Integr. Plant Biol. 52, 904–913.
Jiang, Z.J., Huang, X.P., Zhang, J.P., Zhou, C.Y., Lian, Z.L., Ni, Z.X., 2014. The effects of air exposure on the desiccation rate and photosynthetic activity of *Thalassia hemprichii* and *Enhalus acoroides*. Mar. Biol. 161, 1051–1061.
Jiang, Z., Liu, S., Zhang, J., Zhao, C., Wu, Y., Yu, S., et al., 2017. Newly discovered seagrass beds and their potential for blue carbon in the coastal seas of Hainan Island, South China Sea. Mar. Pollut. Bull. 125, 513–521.
Jiang, Z., Liu, S., Zhang, J., Wu, Y., Zhao, C., Lian, Z., et al., 2018. Eutrophication indirectly reduced carbon sequestration in a tropical seagrass bed. Plant Soil 426, 135–152.
Kenyon, R., Conacher, C., Poiner, I., 1997. Seasonal growth and reproduction of *Enhalus acoroides* (Lf) Royle in a shallow bay in the western Gulf of Carpentaria, Australia. Mar. Freshw. Res. 48, 335–342.
Kim, J.H., Kang, E.J., Kim, K., Jeong, H.J., Lee, K., Edwards, M.S., et al., 2015. Evaluation of carbon flux in vegetative bay based on ecosystem production and CO_2 exchange driven by coastal autotrophs. Algae 30, 121–137.
Lee, K.S., Park, S.R., Kim, Y.K., 2007. Effects of irradiance, temperature, and nutrients on growth dynamics of seagrasses: a review. J. Exp. Mar. Biol. Ecol. 350, 144–175.
Li, R.H., Liu, S.M., Li, Y.W., Zhang, G.L., Ren, J.L., Zhang, J., 2014. Nutrient dynamics in tropical rivers, lagoons, and coastal ecosystems of eastern Hainan Island, South China Sea. Biogeosciences 11, 481–506.
Li, M., Li, R., Cai, W.J., Testa, J.M., Shen, C., 2020. Effects of wind-driven lateral upwelling on estuarine carbonate chemistry. Front. Mar. Sci. 7, 588465.
Lin, H.J., Shao, K.T., 1998. Temporal changes in the abundance and growth of intertidal *Thalassia hemprichii* seagrass beds in southern Taiwan. Bot. Bull. Acad. Sin. 39, 191–198.
Liu, S., Deng, Y., Jiang, Z., Wu, Y., Huang, X., Macreadie, P.I., 2020. Nutrient loading diminishes the dissolved organic carbon drawdown capacity of seagrass ecosystems. Sci. Total Environ. 740, 140185.
Macreadie, P.I., Baird, M.E., Trevathan-Tackett, S.M., Larkum, A.W.D., Ralph, P.J., 2014. Quantifying and modelling the carbon sequestration capacity of seagrass meadows–a critical assessment. Mar. Pollut. Bull. 83, 430–439.
Macreadie, P.I., Anton, A., Raven, J.A., Beaumont, N., Connolly, R.M., Friess, D.A., et al., 2019. The future of blue carbon science. Nat. Commun. 10, 1–13.
Macreadie, P.I., Costa, M.D., Atwood, T.B., Friess, D.A., Kelleway, J.J., Kennedy, H., et al., 2021. Blue carbon as a natural climate solution. Nat. Rev. Earth Environ. 2, 826–839.
Maher, D.T., Eyre, B.D., 2012. Carbon budgets for three autotrophic Australian estuaries: implications for global estimates of the coastal air-water CO_2 flux. Glob. Biogeochem. Cycles 26, GB1032.
Mateo, M.A., Cebrián, J., Dunton, K., Mutchler, T., 2006. Carbon flux in seagrass ecosystems. In: Seagrasses: Biology, Ecology and Conservation. Springer.
Mcleod, E., Chmura, G.L., Bouillon, S., Salm, R., Björk, M., Duarte, C.M., et al., 2011. A blueprint for blue carbon: toward an improved understanding of the role of vegetated coastal habitats in sequestering CO_2. Front. Ecol. Environ. 9, 552–560.
Ollivier, Q.R., Maher, D.T., Pitfield, C., Macreadie, P.I., 2022. Net drawdown of greenhouse gases (CO_2, CH_4 and N_2O) by a temperate Australian seagrass meadow. Estuar. Coasts 45, 2026–2039.
Polsenaere, P., Lamaud, E., Lafon, V., Bonnefond, J.M., Bretel, P., Delille, B., et al., 2012. Spatial and temporal CO_2 exchanges measured by Eddy Covariance over a temperate intertidal flat and their relationships to net ecosystem production. Biogeosciences 9, 249–268.
Rollón, R.N., 1998. Spatial Variation and Seasonality in Growth and Reproduction of Enhalus acoroides (L.f.) Royle Populations in the Coastal Waters off Cape Bolinao, NW Philippines: Submitted in Fulfilment of the Requirements of the Board of Deans of Wageningen Agricultural University and the Academic Board of the International Institute for Infrastructural, Hydraulic and Environmental Engineering for the Degree of Doctor.
Stankovic, M., Ambo-Rappe, R., Carly, F., Dangan-Galon, F., Fortes, M.D., Hossain, M.S., et al., 2021. Quantification of blue carbon in seagrass ecosystems of Southeast Asia and their potential for climate change mitigation. Sci. Total Environ. 783, 146858.
Sutton, A.J., Wanninkhof, R., Sabine, C.L., Feely, R.A., Cronin, M.F., Weller, R.A., 2017. Variability and trends in surface seawater pCO_2 and CO_2 flux in the Pacific Ocean. Geophys. Res. Lett. 44, 5627–5636.
Takahashi, T., Sutherland, S.C., Sweeney, C., Poisson, A., Metzl, N., Tilbrook, B., et al., 2002. Global sea–air CO_2 flux based on climatological surface ocean pCO_2, and seasonal biological and temperature effects. Deep Sea Res. Part II 49, 1601–1622.
Tang, J., Ye, S., Chen, X., Yang, H., Sun, X., Wang, F., et al., 2018. Coastal blue carbon: concept, study method, and the application to ecological restoration. Sci. China Earth Sci. 61, 637–646.
Tokoro, T., Hosokawa, S., Miyoshi, E., Tada, K., Watanabe, K., Montani, S., et al., 2014. Net uptake of atmospheric CO_2 by coastal submerged aquatic vegetation. Glob. Chang. Biol. 20, 1873–1884.
Urbini, L., Ingrosso, G., Djakovac, T., Piacentino, S., Giani, M., 2020. Temporal and spatial variability of the CO_2 system in a riverine influenced area of the Mediterranean Sea, the Northern Adriatic. Front. Mar. Sci. 7, 679.
Van Dam, B.R., Lopes, C., Osburn, C.L., Fourqurean, J.W., 2019. Net heterotrophy and carbonate dissolution in two subtropical seagrass meadows. Biogeosciences 16, 4411–4428.
Van Dam, B., Polsenaere, P., Barreras-Apodaca, A., Lopes, C., Sanchez-Mejia, Z., Tokoro, T., et al., 2021a. Global trends in air-water CO_2 exchange over seagrass meadows revealed by atmospheric Eddy covariance. Glob. Biogeochem. Cycles 35, e2020GB006848.
Van Dam, B.R., Lopes, C.C., Polsenaere, P., Price, R.M., Rutgersson, A., Fourqurean, J.W., 2021b. Water temperature control on CO_2 flux and evaporation over a subtropical seagrass meadow revealed by atmospheric eddy covariance. Limnol. Oceanogr. 66, 510–527.
Vermaat, J.E., Agawin, N., Fortes, M., Uri, J., Duarte, C.M., Marbà, N., et al., 2017. The capacity of seagrasses to survive increased turbidity and siltation: the significance of growth form and light use. Ambio 26, 499–504.
Wanninkhof, R., 2014. Relationship between wind speed and gas exchange over the ocean revisited. Limnol. Oceanogr. Methods 12, 351–362.
Wanninkhof, R., Triñanes, J., 2017. The impact of changing wind speeds on gas transfer and its effect on global air-sea CO_2 fluxes. Glob. Biogeochem. Cycles 31, 961–974.
Weiss, R.F., 1974. Carbon dioxide in water and seawater: the solubility of a non-ideal gas. Mar. Chem. 2, 203–215.
Wimart-Rousseau, C., Lajaunie-Salla, K., Marrec, P., Wagener, T., Raimbault, P., Lagadec, V., et al., 2020. Temporal variability of the carbonate system and air-sea CO_2 exchanges in a Mediterranean human-impacted coastal site. Estuar. Coast. Shelf Sci. 236, 106641.
Wu, P., Han, Y., Tian, M., 2015. The measurement and comparative study of carbon dioxide emissions from tourism in typical provinces in China. Acta Ecol. Sin. 35, 184–190.
Yates, K.K., Dufore, C., Smiley, N., Jackson, C., Halley, R.B., 2007. Diurnal variation of oxygen and carbonate system parameters in Tampa Bay and Florida Bay. Mar. Chem. 104, 110–124.
Zhang, X., Liu, S., Li, J., Wu, Y., Luo, H., Jiang, Z., et al., 2022. Nutrient enrichment decreases dissolved organic carbon sequestration potential of tropical seagrass meadows by mediating bacterial activity. Ecol. Indic. 145, 109576.
Zhou, Y., Liu, X., Liu, B., Liu, P., Wang, F., Zhang, X., et al., 2015. Unusual pattern in characteristics of the eelgrass *Zostera marina* L. in a shallow lagoon (Swan Lake), north China: implications on the importance of seagrass conservation. Aquat. Bot. 120, 178–184.